Control of the hexapod robot's locomotion with the nonlinear stick-slip induced vibrations

Dariusz Grzelczyk*, Bartosz Stańczyk and Jan Awrejcewicz

Abstract: In the paper the control problem of the six-legged walking robot is studied. In order to find the relationship between commonly used by insects gaits (trajectory of the foot point) and stable trajectory of mechanical systems, at first we analyse various previous papers and the gaits of the real insects. For control the motion of the tip of the robot leg a nonlinear mechanical oscillator describing stick-slip induced vibrations as a so-called central pattern generator (CPG) has been proposed. The advantages of the proposed model has been presented and compared with other previous applied mechanical oscillators. The possibility of control of the tip of the robot leg via changing parameters characterized oscillator working as a CPG has been discussed. Time series of the joints and configurations of the robot leg during walking are presented. The obtained numerical solutions indicate some analogies between the characteristics of the simulated walking robot and animals found in nature. Moreover, some aspects of an energy efficiency analysis (in order to reduce the energy costs) are discussed for the analysed system and the whole hexapod robot. In particular, we discuss the interplay of the proposed gait patterns and the system energy cost.

Keywords: hexapod, central pattern generator, stick-slip vibrations

1. Introduction

As it is well known the legged locomotion is very common in nature. Walking multi-legged robots belong to the important group of mobile robots because of mimics the movement of people or animals [1], [2]. One of the most important advantage of the legged movement in comparison of wheeled/tracked movement is the adaptability to different kinds of terrains [3]. Moreover, in comparison with wheeled/tracked locomotion, a multi-legged walking robots machine are widely recognized as a more effective and efficient transportation, in particular on complex terrains [4]. This is why from a viewpoint of application various types of bio-inspired robots are required for satisfactory exploration of the highly broken and unstable landscapes prevailing on other planets [5].

In the case of six legged robots there is an especially great spectrum of various types of gaits. However the control of their legs does not belong to easy task. The six-legged hexapod robot, in general, has superior walking performance in comparison with those with fewer legs in terms of lower control method complexity, greater statical and dynamical stability as well as greater walking speeds. This is the reason that over the last thirty years an extensive research has been conducted in this field and various prototypes of hexapod walking robots have been performed and tested.

As it is well known power is a limited resource in autonomous robots, therefore many researchers explore power consumption optimization techniques for these machines. Moreover, it is well known that power consumption is one of the main operational restrictions on autonomous walking robots [4]. Sometimes, the proper development of walking robots has been limited by the problem of their high energy consumption. A brief literature review regarding to power consumption optimization for walking machines can be found in paper [4]. Based on the literature review [6] - [12] in the mentioned paper, the authors summarize optimization problem of power consumption and energy costs from other point of view, i.e. by optimizing the gait parameters.

Our paper is organized as follows. Biologically inspired mathematical model and performed prototype of the hexapod leg are introduced. Forward and inversed kinematics of the considered mechanism are studied. An oscillator governing stick-slip vibrations for control the tip motion of the robot leg as a (CPG) is proposed. Numerical results are presented and problems regarding the power consumption are discussed.

2. Model of the biologically inspired hexapod leg

Our research work has been preceded by the biological inspiration, the literature review devoted to the six-legged insects occurring in the nature and various methods of control of six-legged robots inspired by these ones. Figure 1 shows schematic diagram of the morphology of a stick insect leg.

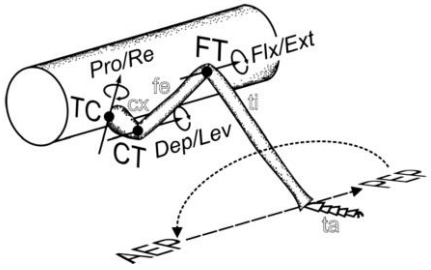

Fig. 1. A scheme of a leg of a stick insect, consisting of four functional segments: coxa (cx), femur (fe), tibia (ti) and tarsus (ta) [13].

The presented leg can be modeled as a manipulator of three segments connected through hinge joints, i.e.: the thorax-coxa joint (TC), the coxa-trochanter joint (CT), and femur-tibia joint (FT) [13]. The dashed lines in Fig. 1 denote swing movement and stance movement. Based on the schematic diagram of a leg of insect we consider a kinematic model and prototype of the constructed leg as is shown in Fig. 2. All of the parts of constructed prototype are designed by aluminum and the actuators are modeled by a standard servomechanisms, which are easy to accomplish position control. Our physical model of the hexapod leg is built up to make the result more convincible in the future work. Applied actuators are standard analog servo-motors controlled via Pulse-Width Modulation (PWM) technique and they are powered independently. The details of the constructed leg are shown in Tab. 1.

The work has been supported by the National Science Foundation of Poland under the grant MAESTRO2 No. 2012/04/A/ST8/00738 for years 2012-2016.

Dariusz Grzelczyk, Bartosz Stańczyk and Jan Awrejcewicz are with the Department of Automation, Biomechanics and Mechatronics, Lodz University of Technology, Lodz, Poland (e-mails: *dariusz.grzelczyk@p.lodz.pl*, *bartosz.stanczyk@dokt.p.lodz.pl*, *jan.awrejcewicz@p.lodz.pl*).

* - corresponding author

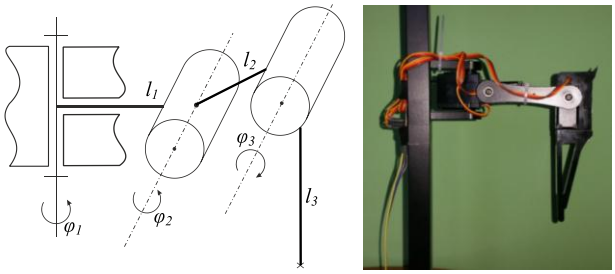

Fig. 2. The kinematic structure and the prototype of the constructed single robot leg. Angle φ_1 describes the angular position of the thorax-coxa joint, angle φ_2 stands for the position of the coxa-trochanterofemur joint, whereas angle φ_3 describes the position of the femur-tibia joint. The lengths of the three links (coxa, femur and tibia) are denoted by l_1, l_2 and l_3, respectively.

Tab. 1. Parameters of the robot leg

Name	Symbol	Value
coxa	l_1	27 mm
femur	l_2	70 mm
tibia	l_3	120 mm
TC joint	φ_1	0 ... 180°
CT joint	φ_2	-90° ... 90°
FT joint	φ_3	0 ... 150°

2.1. Forward kinematics

The presented in Fig. 2 mechanism can be treated as a multibody system. Kinematic description of the multibody system is a recipe for transformation, which describes the geometrical relationship between the generalized coordinates $\mathbf{q}$ and coordinates $\mathbf{x}$ of the global base coordinate system. In general, this relationship has the following non-linear form

$$\mathbf{x} = \mathbf{f}(\mathbf{q}), \tag{1}$$

where $\mathbf{q} = [\varphi_1, \varphi_2, \varphi_3]^T$ and $\mathbf{x} = [x, y, z]^T$. In mechatronic applications a particular importance is to calculate the position of the effector, which is a point important for the realized mechatronic task. In the considered structure we take a tip of the robot leg (foot point) as an effector.

Figure 3 shows the leg of the hexapod for arbitrary configuration in the base global coordinate system. On the basis of Fig. 3, we can determine the forward kinematics taking x, y and z coordinates of the foot point as a function of the lengths l_i, and the angles φ_i, where $i = 1,2,3$.

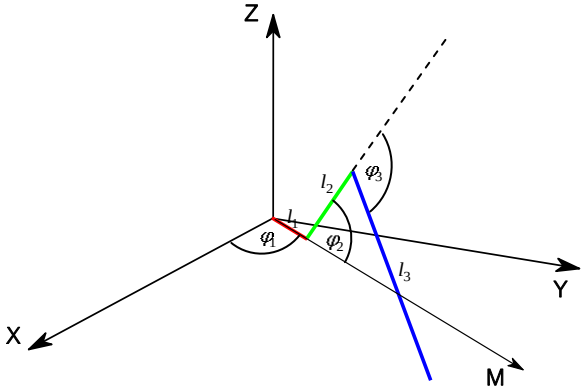

Fig. 3. Location of the hexapod leg in the global base coordinate system.

Taking into account $\cos(\theta_3 - \theta_2) = \cos\theta_2 \cos\theta_3 + \sin\theta_2 \sin\theta_3$ and $\sin(\theta_3 - \theta_2) = \sin\theta_3 \cos\theta_2 - \cos\theta_3 \sin\theta_2$ we get

$$\begin{cases} x = \cos\varphi_1(l_1 + l_2\cos\varphi_2 + l_3\cos\varphi_2\cos\varphi_3 + l_3\sin\varphi_2\sin\varphi_3), \\ y = \sin\varphi_1(l_1 + l_2\cos\varphi_2 + l_3\cos\varphi_2\cos\varphi_3 + l_3\sin\varphi_2\sin\varphi_3), \\ z = l_2\sin\varphi_2 - l_3\cos\varphi_2\sin\varphi_3 + l_3\sin\varphi_2\cos\varphi_3. \end{cases} \tag{2}$$

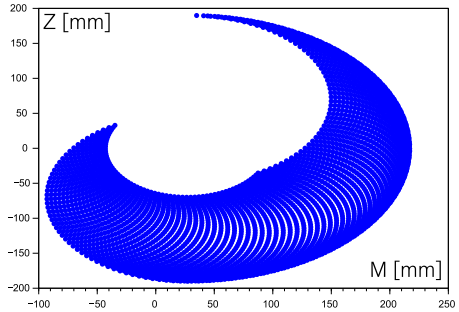

Fig. 4. Workspace of the haxapod foot point.

Figure 4 shows the workspace of the flat considered mechanism of the robot leg (in the plane of this mechanism) for parameters shown in Tab. 1.

2.2. Inverse kinematics

In the inverse kinematics we are looking for the appropriate generalized coordinates $\mathbf{q}$ as a function of the global coordinates $\mathbf{x}$, in order to keep the correct configuration of the system. Formally, we obtain the inverse relationship

$$\mathbf{q} = \mathbf{f}^{-1}(\mathbf{x}), \tag{3}$$

which usually is strongly nonlinear, and analytically solutions can be obtained only in special cases.

In our studies inverse kinematics has been determined using the appropriate trigonometry relations. Through the analyzing of the robot's leg mechanism shown in Fig. 3, it can be seen that the angle φ_1 is decoupled from other angles φ_2 and φ_3, and we have

$$\varphi_1 = \begin{cases} \arctan\left(\dfrac{y}{x}\right) & \text{if} \quad x \geq 0, \\ \pi - \arctan\left(\dfrac{y}{-x}\right) & \text{if} \quad x < 0. \end{cases} \tag{4}$$

In order to obtain relations on angles φ_2 and φ_3, we take into consideration the mechanism of the robot leg lying in a plane defined by this mechanism and shown in Fig. 5.

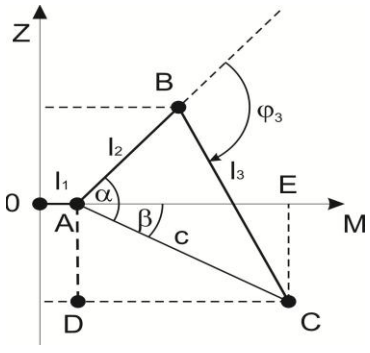

Fig. 5. Projection of the robot leg in the plane $Z-M$ defined by the considered mechanism.

For the right-angled triangle ACD the Pythagorean theorem takes the form

$$z^2+\left(\sqrt{x^2+y^2}-l_1\right)^2=c^2. \tag{5}$$

In turn, for the triangle ABC the cosine theorem yields

$$c^2=l_2^2+l_3^2-2l_2l_3\cos(\pi-\varphi_3). \tag{6}$$

Taking (5), (6) and relation $\cos(\pi-\varphi_3)=-\cos\varphi_3$ the following formula is obtained

$$\cos\varphi_3=\frac{c^2-l_2^2-l_3^2}{2l_2l_3}, \tag{7}$$

where $c=\sqrt{z^2+\left(\sqrt{x^2+y^2}-l_1\right)^2}$. Finally a relation regarding the angle φ_3, has the following form

$$\varphi_3=\arccos\left(\frac{c^2-l_2^2-l_3^2}{2l_2l_3}\right), \tag{8}$$

where $c=\sqrt{z^2+\left(\sqrt{x^2+y^2}-l_1\right)^2}$.

In order to obtain the relation on angle φ_2 ,we consider again the triangle ABC and the cosine theorem as follows

$$l_3^2=l_2^2+c^2-2l_2c\cos\alpha. \tag{9}$$

Finally, taking (9) we have

$$\alpha=\arccos\left(\frac{l_3^2-l_2^2-c^2}{-2l_2c}\right). \tag{10}$$

Due to the real constraints of our mechanical system and the definition of the angle φ_3, the value of the mentioned angle φ_3 can not be negative (see Tab. 1). Accordingly, the angle α will take always positive values. In turn, taking the right-angled triangle ACE, we get

$$\tan(-\beta)=\frac{-z}{\sqrt{x^2+y^2}-l_1}\Rightarrow\beta=\arctan\left(\frac{z}{\sqrt{x^2+y^2}-l_1}\right). \tag{11}$$

Values of β can be both positive or negative. If $\sqrt{x^2+y^2}-l_1\geq 0$, then $\varphi_2=\alpha+\beta$. In turn, if $\sqrt{x^2+y^2}-l_1<0$, then $\varphi_2=\alpha-(\pi-\beta)$. Finally the inverse kinematic of the considered system has the following form

$$\begin{aligned}
\varphi_1&=\begin{cases}\arctan\left(\frac{y}{x}\right) & \text{if} \quad x\geq 0,\\ \pi-\arctan\left(\frac{y}{-x}\right) & \text{if} \quad x<0.\end{cases}\\
\varphi_2&=\begin{cases}\alpha+\beta & \text{if} \quad \sqrt{x^2+y^2}-l_1\geq 0,\\ \alpha-(\pi-\beta) & \text{if} \quad \sqrt{x^2+y^2}-l_1<0,\end{cases}\\
\varphi_3&=\arccos\left(\frac{c^2-l_2^2-l_3^2}{2l_2l_3}\right),
\end{aligned} \tag{12}$$

where $\alpha=\arccos\left(\frac{l_3^2-l_2^2-c^2}{-2l_2c}\right)$, $\beta=\arctan\left(\frac{z}{\sqrt{x^2+y^2}-l_1}\right)$ and $c=\sqrt{z^2+\left(\sqrt{x^2+y^2}-l_1\right)^2}$.

3. Central pattern generators

In our investigations we use the traditional method to control the hexapod robot's leg by planning out the foot point trajectory and the velocity for transfer phase and support phase in the working space. In this method the shape of the trajectory of the foot point of the robot leg is generated by the central pattern generator (CPG). As CPG vibrations of linear or nonlinear dynamical systems with stable orbits in the phase space are usually used and applied. Next, the appropriate position of the phase trajectories of the individual points are converted to joint space using the inversed kinematics. Finally, the corresponding joint angles give a predetermined trajectory of the tip of the robot leg in the workspace by the employed forward kinematics.

There are numerous models to generate the central oscillation presented in the literature. Through a brief literature review analysis, below we present some chosen oscillators applied to control leg's mechanism. In most of them the reported limit cycles are asymptotically stable. The CPG model was first proposed by Cohen, Holmes and Rand in 1980s through the study on the dissection of a lamprey spinal cord [14]. Since this time, numerous researchers apply the CPG algorithms to the control of bio-inspired robots. For instance, as a CPG linear damped or non-damped harmonic oscillations, non-linear Van der Pol or Rayleigh oscillators, and Toda-Rayleigh lattice have been used and applied by many researches [15].

A brief literature review on the implementation of CPG algorithms to control of hexapod movement can be found in papers [3], [15], or in the review paper [16]. The common point of the presented CPG models is that represent various kinds of linear or nonlinear dynamical systems. In paper [17], different oscillators and similarities/differences between them have been discussed. In the paper [18] several oscillators have been coupled together to construct the CPG model. The controlled in this way robot can walk on the land and swim in the water. In turn, the paper [19] show that hexapod robot can perform different kinds of gaits by chaos control (however, the proposed model is difficult to be directly applied).

Different types of oscillators used as CPG give different gaits of the robot. Transition between various gaits should has a smooth character. This problem is considered in the paper [3], which focuses on the topic of smooth gait transition of a hexapod robot by a proposed central pattern generator algorithm. In the mentioned paper CPG is constructed by an isochronous oscillators and several first-order low-pass filters.

4. Numerical results

All presented below numerical results have been obtained via fourth order Runge-Kutta method implemented in Scilab for constant time step $h=0.01$. First, as an example of the previous used nonlinear systems serving as a CPG, we

consider the mentioned earlier Van der Pol and Rayleigh oscillators. Van der Pol oscillator is described by the following nonlinear ordinary differential equation (ODE)

$$\ddot{X} - \mu(1 - X^2)\dot{X} + \omega^2 X = 0. \qquad (13)$$

The solution of this equation has a limit cycle in phase space and can be used to generate the trajectory of the hexapod foot point. The frequency of the vibrations can be controlled via parameter ω. Figure 6 shows limit cycles of the considered oscillator for various values of the parameter μ, and phase portraits obtained for fixed values of the parameters $\mu = 8$, $\omega = 2$, and various initial conditions.

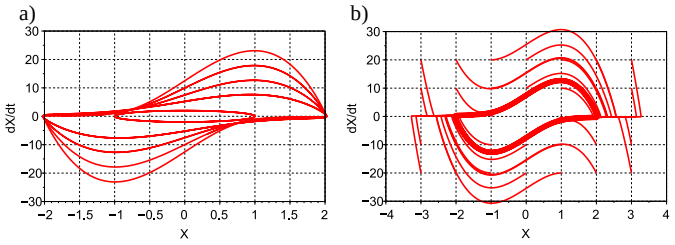

Fig. 6. Phase trajectories of the Van der Pol oscillator: a) for various μ; b) for various initial conditions (stable trajectory has been bolded).

As a second example we consider the Rayleigh oscillator described by the following nonlinear ODE

$$\ddot{X} - \mu(1 - \dot{X}^2)\dot{X} + \omega^2 X = 0. \qquad (14)$$

Also in this case this equation has a limit cycle in phase space, and the parameter ω controls the frequency of the vibrations. Figure 6 shows limit cycles of the considered oscillator for various values of the parameter μ, and the phase portraits obtained for $\mu = 8$, $\omega = 2$ and various initial conditions.

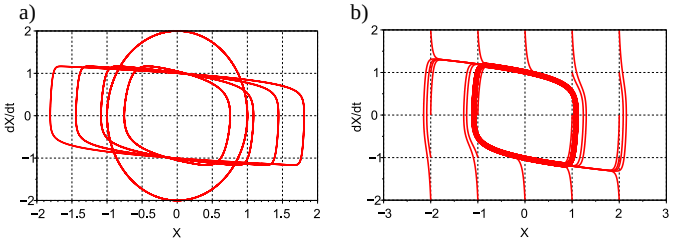

Fig. 7. Phase trajectories of the Rayleigh oscillator: a) for various μ; b) for various initial conditions (stable trajectory has been bolded).

Figures 6 and 7 show the possibility of change of the generated trajectory by parameter μ as well as a stability of the obtained solutions (the same limit cycle for various initial conditions). Observe that in both cases of either Van der Pol or Rayleigh oscillator, for $\mu = 0$, we have linear, non-dumped and non-excited oscillations presented in Figs. 6 and 7.

Below we use two above oscillators to control of the tip of the robot leg. The obtained stable orbits as a CPS signals have been scaled to the workspace of the robot leg, and next converted to the joint space by the inverse kinematics. Variable X of the oscillator is used to control the robot foot point in the direction of the X-axis, variable $\dot{X}$ is used to control in the Z-direction, while the variable y of the robot leg is constant. Figure 8 shows time series of angles φ_1, φ_2 and φ_3. In order to obtain a stable trajectory of the Van der Pol oscillator ($\mu = 4$, $\omega = 2$), we apply $X(0) = 0$, $\dot{X}(0) = 1$. The obtained orbit has been scaled to the workspace. Moreover, the obtained (in this way) trajectory of the foot point and the chosen configurations of the robot leg have been reported in Fig. 9.

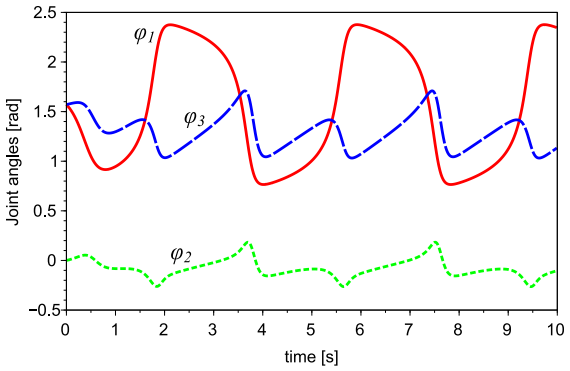

Fig. 8. Time series of angles φ_1, φ_2 and φ_3 obtained for the Van der Pol oscillator.

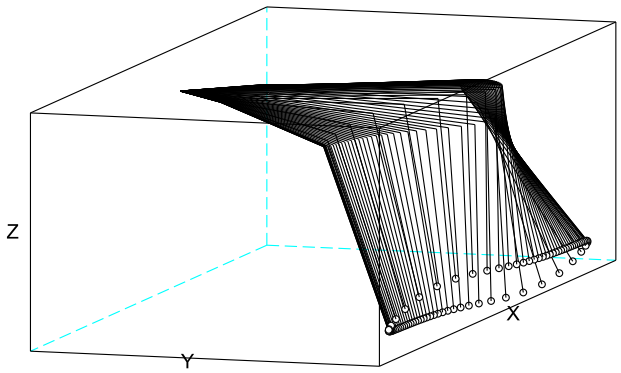

Fig. 9. Visualization of the robot leg configurations and plotting the Van der Pol trajectory by the tip of the robot leg.

Figure 10 shows time series of angles φ_1, φ_2 and φ_3 using the stable trajectory of the Rayleigh oscillator for $\mu = 4$, $\omega = 2$, and initial conditions $X(0) = 0$, $\dot{X}(0) = 1$. The obtained orbit has been scaled to the workspace. Trajectory of the foot point and chosen configurations of the robot leg have been reported in Fig. 11.

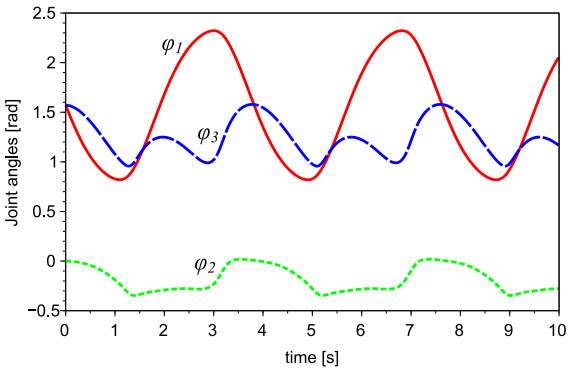

Fig. 10. Time series of angles φ_1, φ_2 and φ_3 obtained for the Rayleigh oscillator.

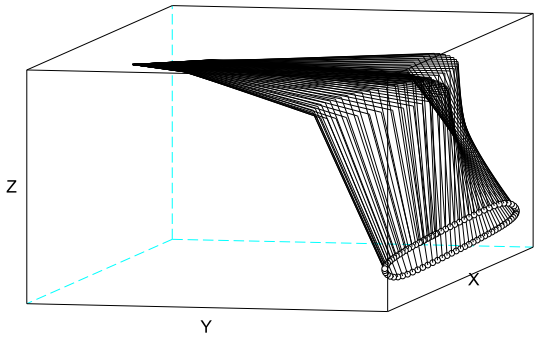

Fig. 11. Visualization of the robot leg configurations and plotting the Rayleigh trajectory by the tip of the robot leg.

The presented above results show the correct mathematical description of the forward and inverse kinematics of the considered mechanism, as well as the ability to apply these oscillators to control of the tip of the robot leg. Presented in this way time series of angles φ_1, φ_2 and φ_3 allow us to assess the possibility of obtaining of the planned trajectory. The tip of the robot leg is able to plotting the planned trajectory if angles φ_1, φ_2, φ_3 belong to the intervals given in Tab. 1.

Application of nonlinear oscillators described so far provides a relatively easy way to control of the tip of the robot leg. Changing of the gait parameters can be achieved by changing the parameters of the oscillators applied as a CPG. However, as can be seen based on the presented leg's configurations, during walking a distance between foot point and center of the robot coordinate system positioned on the body of the robot at the point of attachment leg changes significantly. This is a result of cyclically shifting up and down the center of gravity of the robot. In this way, the servos placed in leg joints robot must perform extra unnecessary work, which significantly increases the energy demand for the used servos.

Motivated by the carried out study of the trajectory of the tip of a biologically inspired robot legs (Fig. 1), and in order to control of the robot leg tip, other nonlinear mechanical oscillator has been proposed. The trajectory of the mentioned oscillator has a shape similar to the shape of the trajectory of the tip of the robot leg shown in Fig. 1 (see dashed lines). For this reason, as a CPG 1-DOF mechanical system with stick-slip induced vibrations is proposed and analysed. The proposed model is governed by the following non-dimensional equation

$$\ddot{X} + d\dot{X} + X = F_{fr}(v_r). \tag{15}$$

In equation (15) d denotes non-dimensional damping coefficient, and $F_{fr}(v_r) = \dfrac{F_s}{1+\delta\,|v_r|}\operatorname{sgn}(v_r)$ is a non-dimensional dry friction force, which depends on the non-dimensional relative sliding velocity $v_r = v_{dr} - \dot{X}$ with respect to the constant velocity v_{dr}. Parameters F_s and δ characterize the function $F_{fr}(v_r)$. In our numerical calculations non-smooth signum function $\operatorname{sgn}(v_r)$ has been approximated by the smooth and often applied hyperbolic tangent function of the following form

$$\operatorname{sgn}(v_r) = \tanh\left(\frac{v_r}{\varepsilon}\right) \tag{16}$$

with control parameter ε. The individual parameters of the proposed model have essential influence on the oscillation frequency and the shape of the obtained phase trajectories. For further studies, as an example, we consider stable orbits of the proposed CPG model obtained for the parameters $d = 0.01$, $F_s = 1$, $\delta = 3$, $v_{dr} = 0.5$, and the control parameter $\varepsilon = 10^{-2}$. Figure 12 presents the obtained stable cycles for various initial conditions. In each of the cases we obtain stable phase trajectories, also for zeros initial conditions.

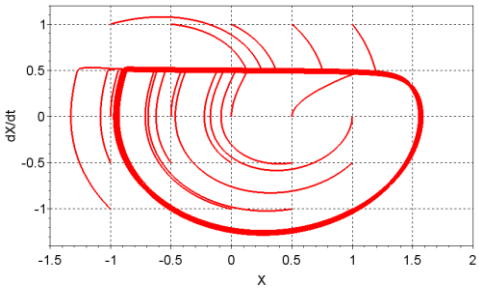

Fig. 12. Stable phase trajectories of the mechanical stick-slip oscillator for various initial conditions (stable trajectory has been bolded).

The obtained stable orbit has been scaled to the working space of the robot leg by multiplying variable X and scale coefficient equal to -100, as well as multiplying variable $\dot{X}$ and scale coefficient equal to -10. Based on the relation (12), the time series of angles φ_1, φ_2 and φ_3 has been obtained and presented in Fig. 13. Moreover, trajectory of the foot point and chosen configurations of the robot leg have been also reported in Fig. 14.

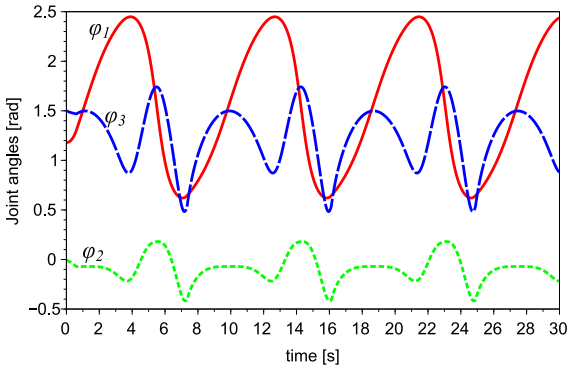

Fig. 13. Time series of angles φ_1, φ_2 and φ_3 obtained for the stick-slip oscillator.

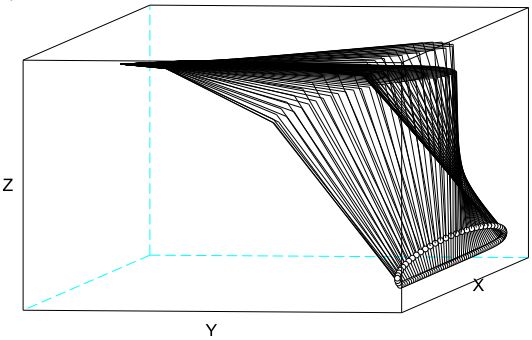

Fig. 14. Visualization of the robot leg configurations and plotting the stick-slip trajectory by the tip of the robot leg.

As can be seen, the tip of the robot leg starts from initial configuration (zeros initial conditions of the CPG) plotting a stable trajectory in the workspace. The obtained trajectory lies in the plane parallel to the X-axis. Moreover, the distance between foot point and center of the robot coordinate system positioned on the body of the robot at the point of attachment leg is constant. In fact, this is a result of keeping the center of gravity of the robot at a constant level. Finally, the servos placed in leg joints robot don't have to perform extra work, which significantly decreases the energy demand. For better understanding of this issue also distance of the foot point to the ground has been reported (Fig. 15).

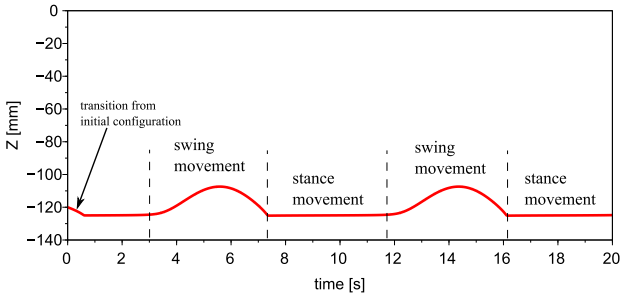

Fig. 15. The distance of the foot point to the ground.

5. Conclusions and future studies

In the paper we use the traditional method to control the hexapod robot's leg by planning out the foot point trajectory and the velocity for transfer phase and support phase in the workspace. Kinematic scheme, constructed prototype and mathematical description of the both forward and inverse kinematics biologically inspired and considered mechanism have been presented in detail. Two different nonlinear oscillators have been applied as a CPG, and finally non-linear stick-slip induced vibrations as a CPG algorithm controlling of the hexapod leg in the workspace has been proposed.

Through the performed numerical analysis, we can draw the following main concluding remarks:

1. There are two approaches to accelerate the robot movement: increasing the free frequency of oscillations or enlarging the amplitude of the foot point during conversion of the CPG orbit to the working space by scaling CPG's variables in order to generate a larger stride for the robot. Various scale coefficients on different sides of the hexapod body allow to change the direction of its movement.
2. The presented numerical results (configurations of the robot leg, and trajectories plotted by the tip of leg) show good analogies between the gait of the simulated walking robot and the gaits of animals in nature.
3. It can be seen, based on the presented time series of angles of the appropriate joints, that the control system must activate some muscles twice for each stepping cycle.
4. Our proposed CPG algorithm being based on the stick-slip induced vibrations, can be more energy efficiently in comparison to other used and applied CPG models.
5. Amplitude of the oscillation of the foot point in the working space (both in X and Z direction) can be controlled independently by the easy scaling of the CPG orbits.
6. It should be emphasized that the presented algorithm based on the stick-slip vibrations is not demanding from a numerical point of view, i.e. suitable trajectories are obtained for extremally large numerical parameters (step time and control parameter ε).

However, it should be noted that using the proposed algorithm, the precise description of the considered mechanical model is necessary. Moreover, it should also be noted that if a leg gets stuck by an obstacle, the robot should to stop the leg, detect the current orientation and position, and recalculate new trajectory. For this reason some sensor information should be employed, for instance piezoelectric sensors on the foot point, working as a feedback.

In our future studies regarding an energy consumption of a robot the sum of the energy consumed in all of the joints will be considered. We are going to use a model of a DC motor and a gear system of applied servomechanism in the joint of the leg for obtaining the power consumption experimental data from the required voltage and current values.

References

1. T. Zielińska, "Biological inspiration used for robots motion synthesis", *Journal of Phisiology*, Vol. 103, pp. 133-140, 2009.
2. T. Zielińska, C.M. Chew, P. Kryczka and T. Jargilo, "Robot gait synthesis using the scheme of human motion skills development", *Mechanism and Machine Theory*, Vol. 44(3), pp. 541-558, 2009.
3. W. Chen, G. Ren, J. Zhang and J. Wang, "Smooth transition between different gaits of a hexapod robot via a central pattern generators algorithm", *J Intell Robot Syst*, Vol. 67, pp. 255–270, 2012.
4. B. Jin, C. Chen and W. Li, "Power consumption optimization for a hexapod walking robot", *J Intell Robot Syst*, Vol. 71, pp. 195–209, 2013.
5. R. Altendorfer, N. Moore, H. Komsuoglu, M. Buehler, H.B. Brown jn., D. McMordie, U. Saranli, R. Full and D.E. Koditschek, "Hex: a biologically inspired hexapod runner", *Autonomous Robots*, Vol. 11, pp. 207–213, 2001.
6. M.S. Erden, "Optimal protraction of a biologically inspired robot leg", *J Intell Robot Syst*, Vol. 64(3,4), pp. 301–322, 2011.
7. J. Nishii, "Legged insects select the optimal locomotor pattern based on the energetic cost", *Biol. Cybern.*, Vol. 83, pp. 435–442, 2000.
8. J. Nishii, "An analytical estimation of the energy cost for legged locomotion", *J. Theor. Biol.*, Vol. 238, pp. 636–645, 2006.
9. T.A. Guardabrazo and P. Gonzalez de Santos, "Building an energetic model to evaluate and optimize power consumption in walking robots", *Ind. Robot*, Vol. 31(11), pp. 201–208, 2004.
10. P. Gonzalez de Santos, E. Garcia, R. Ponticelli, M. Armada, "Minimizing energy consumption in hexapod robots", *Adv. Robot.*, Vol. 23, pp. 681–704, 2009.
11. E. Garcia, J.A. Galvez and P. Gonzalez de Santos, "On finding the relevant dynamics for model-based controlling walking robots", *J. Intell. Robot. Syst.*, Vol. 37, pp. 375–398, 2003.
12. P. Gonzalez de Santos, J. Estremera and E. Garcia, "Optimizing leg distribution around the body in walking robots" [in:] Proceedings of the 2005 IEEE International Conference on Robotics and Automation, Barcelona, Spain, 2005.
13. V. Durr, J. Schmitz and H. Cruse, "Behaviour-based modelling of hexapod locomotion: linking biology and technical application", *Arthropod Struct Dev.*, Vol. 33(3), pp. 237–250, 2004.
14. A. Cohen, P. Holmes and R. Rand, "The nature of the coupling between segmental oscillators of the lamprey spinal generator or locomotion: a mathematic model", *J. Math. Biol.*, Vol. 13, pp. 345–369, 1982.
15. M. Piątek, "Robot's control problems - central pattern generators", Doctoral thesis - supervisor Andrzej Turnau, University of Mining and Metallurgy, Krakow, Poland, 2012, 163 pages (in Polish).
16. A. Ijspeert, "Central pattern generators for locomotion control in animals and robots: a review", *Neural Netw.*, Vol. 21(4), pp. 642–653, 2008.
17. J. Buchli, L. Righetti, A. Ijspeert, "Engineering entrainment and adaptation in limit cycle systems—from biological inspiration to applications in robotics", *Biol. Cybern.*, Vol. 95(6), pp. 645–664, 2006.
18. A. Ijspeert, A. Crespi, D. Ryczko and J. Cabelguen, "From swimming to walking with a salamander robot driven by a spinal cord model", *Science*, Vol. 315(5817), pp. 1416–1420, 2007.
19. S. Steingrube, M. Timme, F. Wörgötter and P. Manoonpong, "Self-organized adaptation of a simple neural circuit enables complex robot behaviour", *Nat. Phys.*, Vol. 6, pp. 224–230, 2010.